INSTITUTE OF PHYSICS PUBLISHING JOURNAL OF PHYSICS: CONDENSED MATTER

J. Phys.: Condens. Matter **15** (2003) S3311–S3335 PII: S0953-8984(03)70841-8

Vicinal metal surfaces as nanotemplates for the growth of low-dimensional structures

K Kuhnke[1] **and K Kern**

Max-Planck-Institut für Festkörperforschung, Heisenbergstraße 1, D-70569 Stuttgart, Germany

E-mail: k.kuhnke@fkf.mpg.de

Received 22 October 2003
Published 14 November 2003
Online at stacks.iop.org/JPhysCM/15/S3311

Abstract

Vicinal surfaces, which exhibit a regular array of steps, introduce defined arrangements of surface defects, which have the potential to create specific functionalities of the surface. In particular they can be used as templates for the growth of one-dimensional structures using selective step decoration. In this article we discuss the properties of vicinal metal surfaces and how they can be used as nanotemplates. The requirements for the growth of low-dimensional adsorbate structures at step edges of the vicinal (997) and (779) surfaces of platinum will be discussed in detail. Here energetics determined by the different adsorption sites and the kinetics present through the diffusion processes play an essential role. In order to obtain stable arrangements the propensity of the elements for alloy formation must be taken into account. Examples for the properties of the structures obtained and their role in studying one-dimensional systems are discussed, and we give a short outlook on how the principles of step decoration might be extended to a kind of atomic assembly of more complex surface nanostructures.

1. Introduction

A growing number of surface science and nanoscience publications are devoted to studies of vicinal surfaces. These are surfaces with a high density of substrate steps possibly arranged in a regular step structure. Being close to the morphology of low-index surfaces, vicinal surfaces define a path from nominally defect-free surfaces towards a more complicated surface structure introducing periodic defects at distances significantly larger than the substrate lattice constant. From the point of functionality these defects may—even at low concentration—dominate certain surface properties and processes, for example adsorption and chemical reaction. Vicinal surfaces allow introduction of functional centres in a controlled way. Experimentally, they have the advantage that high-resolution diffraction methods like x-ray scattering, electron diffraction

[1] Author to whom any correspondence should be addressed.

0953-8984/03/473311+25$30.00

or molecular beam diffraction can still be applied because the notion of the surface unit cell remains in many cases an applicable concept. This holds in cases where the defects are arranged in a quasi-periodic way with small deviations from perfect periodicity.

It is possible to prepare vicinal surfaces with a periodic step arrangement on the nanometre scale. Such surfaces are ideally suited as templates for building more complex structures on top of them. This opportunity is of substantial fundamental and technological interest. The size reduction in magnetic storage media and in electronic circuits tends to approach dimensions below 100 nm and as a result the future applicability to information technology has become one of the motivations in this field of research. The creation of one-dimensional atomic clusters or rows opens up the possibility to study the properties of materials at the atomic size limit while the structures exhibit a significant surface density over macroscopic length scales. Last but not least, the field of heterogeneous catalysis research may profit from techniques that allow fabricating surfaces with specific adsorption sites, which have a defined local environment.

For the preparation of structures with lengths of a few nanometres classical top-down strategies fail. On the other hand a serial assembly of surface structures by scanning probe based atomic manipulation—even with arrays of tips—is clearly unfeasible when macroscopic samples have to be prepared as in technological applications. Surface templates offer the opportunity to prepare large areas with identical nanometre structures within a small number of fabrication steps by using surface processes; these have been studied intensely in the field of surface science during recent decades. Similarly to the use of growth processes for the simultaneous generation of nanometre structures, the surface template itself is also obtained in a few-step process. A vicinal metal surface can be prepared by cutting and polishing a single crystal followed by ultra-high vacuum methods like ion beam sputtering for metals. In the case of the semiconductor Si wet chemical treatment (etching) can also be employed.

In this paper we review aspects of the preparation of sub-nanometre structures, which exhibit surface properties which are different from those on low-index surfaces. We investigate the thermodynamic requirements for obtaining certain structures on the basis of the material parameters, and give examples of the properties obtained. Of interest are both the properties of the template and the adsorbate structure.

Studies on a wide variety of vicinal metal surfaces can be found in the literature; for a comprehensive article see e.g. [1] and references therein. With a total of several hundred publications, a complete list of references is beyond the scope of this article. We try to give the relevant references but have to omit numerous important contributions. Substantial effort was devoted to the study of vicinal surfaces with different miscut angles of Cu((111), (001), (110)), Au((001), (111)), Ni((001), (111), (110)), Ag((100), (011), Pt((111)), and vicinal surfaces of the bcc metals Mo((110), (100), (111)) and W((110), (001)). The majority of these clean surfaces were found to be stable with respect to faceting (an exception is e.g. Cu(997) [2]) but only for a few of them were detailed parameter sets like step distance distributions determined.

Special topics of interest which we do not discuss in detail here are the properties of so-called vicinal surfaces with 'magic' step lengths which are obtained for surfaces vicinal to low-index surfaces which exhibit reconstruction [3, 4], vicinal surfaces of bulk alloy crystals [5, 6], processes of step doubling [7, 8] and faceting induced by gas adsorption [9, 10] and thin film deposition [11].

The paper is structured as follows. Section 2 discusses basic aspects of stability of vicinal surfaces, which shall be used as templates. The focus will be on the Pt(997) and Pt(779) surfaces. Section 3 covers the growth on vicinal templates, especially the process of step decoration and the morphology during growth. The section starts from general aspects (section 3.1), proceeds to homoepitaxy on Pt(997) (section 3.2) and presents detailed examples of heteroepitaxy (section 3.3). It addresses the growth of more complex structures composed

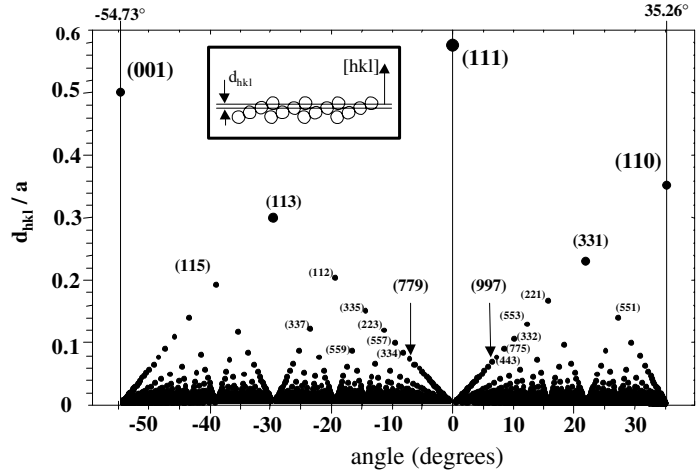

Figure 1. The distance d_{hkl} between the crystallographic layers for surfaces of fcc crystals as a function of miscut angle with respect to the (111) surface. The length scale is given with respect to the fcc bulk lattice constant a. The chosen azimuth covers the important low-index surfaces fcc(001), fcc(110), and the orientations between them. The inset illustrates that the crystallographic layer distance given by equation (1) is determined with respect to the macroscopic surface plane. Thus, on a vicinal surface, atoms of different layers are exposed to the vacuum.

of several adsorbates arranged as sandwiches of monatomic rows at the step edge (section 3.4). At the end (section 3.5) we give a short overview of specific properties of vicinal surfaces with decorated steps and discuss the growth of thicker layers on vicinal surfaces. Section 4 gives an outlook on extensions of the concept, which can lead to the preparation of more complex structures.

2. The stability of vicinal surfaces

Vicinal surfaces are defined as surfaces with surface planes which are in angle close to low-index crystallographic planes. Low-index surfaces are indicated by surface layers with high atomic density in the topmost layer and low nominal defect densities. It is for these reasons that they represent comparatively simple entities that have been studied extensively in the past. From basic crystallography [12] it is known that the distance between crystallographic planes for a surface denoted (hkl) is given by

$$d_{hkl} = \frac{1}{|ha^* + kb^* + lc^*|} \tag{1}$$

where a^*, b^*, c^* are the basis vectors of the reciprocal crystal lattice and h, k, l are the indices of the surface plane (hkl).

In figure 1 we plot the interlayer distance of face centred cubic (fcc) crystallographic planes of the form (hhl) with $0 \leqslant h, l \leqslant 100$ as a function of their angle with respect to the (111) plane. The distance between atomic layers is measured perpendicular to the surface as shown in the inset in figure 1. As we expect, the low-index surfaces (100), (111), and (011) along the chosen azimuth appear at prominent positions in figure 1. The high surface density of atoms in low-index surfaces is directly related to the large distance between atomic layers in the surface plane. What is striking in the plot is the strongly discontinuous nature of the plotted function. Next to each low-index surface one finds exclusively surfaces with layer distances of

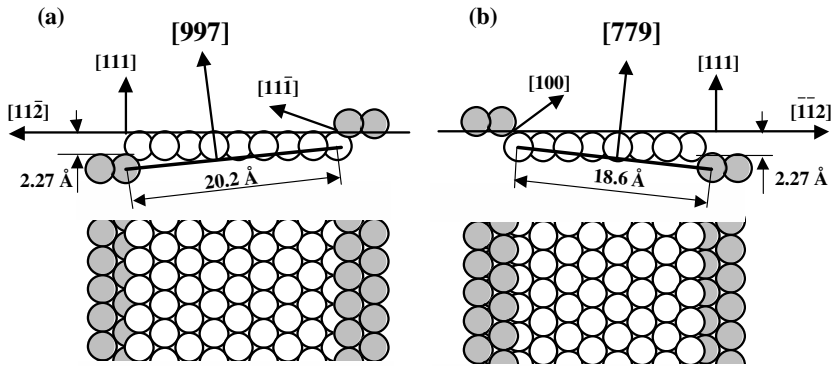

Figure 2. Atom models and length scales of (a) the vicinal Pt(997) and (b) the Pt(779) surface. The top shows the side view of the surface atoms, the bottom shows a top view.

zero even though in experiment these surfaces can hardly be distinguished from the low-index surface itself. Their defect density is still low. In principle, the surfaces vicinal to fcc(111) show a linear increase in the density of monatomic steps when one moves away from the 0° position. The exposed surface of a vicinal surface consists of atoms belonging to different crystallographic layers. The plot helps to illustrate that the addition of a crystallographic layer to a vicinal surface corresponds to the addition of one atom at each defect site. If we take as an example the fcc (997) surface, we find a crystallographic layer distance of 0.069 bulk lattice constants. This is about 1/8 of the (111) layer distance of 0.577 bulk lattice constants. In fact, the fcc (997) surface exhibits a step-terrace structure in which 8 rows of atoms are exposed per repeat unit as sketched in figure 2(a). The terrace of this surface is formed by the (111) close-packed structure of the nearest low-index surface fcc (111) and the step (in the literature often called B-type step) is formed by a (111) microfacet. The fcc (779) surface (figure 2(b)) has a similar terrace structure, however, with (100) microfacet steps (often called A-type steps). The type of step microfacets can be derived from the surface structure of the low-index surface obtained when the angle is increased further. It is seen from figure 1 that increasing the miscut angle for the (997) surface one arrives at the (110) surface structure which consists of alternating close-packed microfacets and increasing the miscut for (779) one approaches the (100) surface.

If we regard homoepitaxial growth on the vicinal surfaces it becomes obvious that the addition of one crystallographic atomic plane is sufficient to exactly recover the initial surface morphology. It is not necessary to cover the entire surface by a new layer. The periodicity in the growth process is thus related to the crystallographic layer density. As diffraction methods are sensitive to periodic oscillations of surface morphology they may follow the formation of rows on vicinal surfaces, given that they are sensitive enough and the morphology changes in an oscillatory way. The reflectivity maxima indicating complete step decoration with adsorbates have been employed for He scattering to monitor the growth of metals on vicinal surfaces [13]. Also other surface and structure sensitive techniques, like surface x-ray scattering and SPA-LEED, may be able to follow the completion of deposited rows on vicinal surfaces. It is for example possible to observe the deposition of one Ag row on Pt(997) in surface x-ray scattering as a shoulder in the intensity on a surface truncation rod in between substrate peaks [14].

The thermodynamics of vicinal surfaces was and still is the subject of numerous theoretical and experimental studies. For a more detailed theoretical introduction we refer the reader for example to [15]. Here we only pick out a few aspects which are of relevance for the following

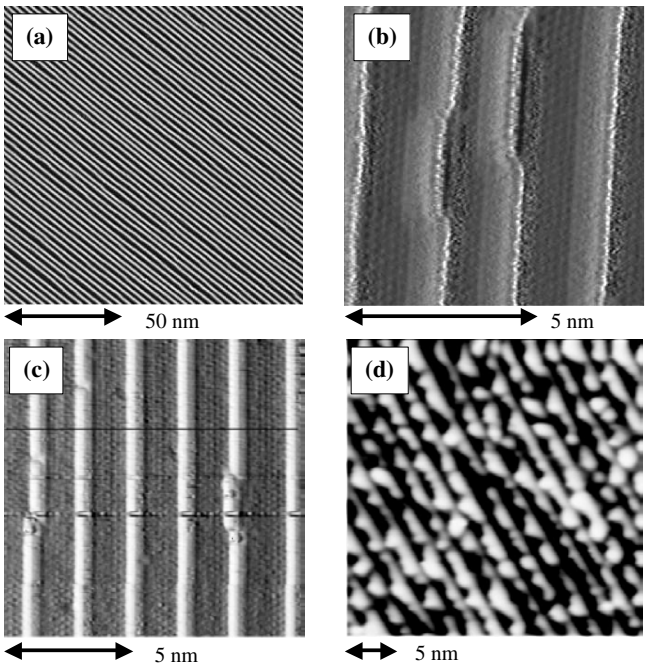

Figure 3. (a) STM image of the clean Pt(997) surface. (b)–(c) Decoration of the substrate step by Ag at 340 K: (b) Ag coverage 0.04 ML, (c) Ag coverage 0.14 ML. (d) The step decoration becomes incomplete when Ag is deposited at 120 K, here shown for a 0.5 ML coverage.

discussions. Vicinal surfaces are in the low-temperature limit metastable structures as the high defect density increases the surface energy above the value of low-index surfaces. This fact may suggest a basic tendency towards faceting, i.e. the phase separation of the vicinal surface into macroscopic regions of low-index surfaces (with a larger total surface area). The vicinal surface can, however, increase its stability through the relaxation of atom positions near the steps [9, 16]. In addition, the observed stability of metallic vicinal surfaces may be due to the preparation pathway, which prevents substantial mass transport from taking place. A typical preparation procedure for a metal single crystal would be given as follows. A single crystal is cut at an angle of a few degrees with respect to a low-index plane. The surface is then polished to yield a surface roughness below 30 nm and finally prepared in vacuum in cycles of rare-gas ion sputtering and annealing to elevated temperatures. Annealing temperatures well below the melting temperature limits surface mass transport, which may result in the creation of low-index facets. The preparation procedure, however, cannot prohibit the formation of mesoscopic facets if they are energetically favoured, and it becomes clear that additional mechanisms must exist if the preparation renders well ordered vicinal surfaces. Figure 3(a) shows a scanning tunnelling microscopy (STM) image of a Pt(997) surface prepared in the way just described. The microscopic structure model is given in figure 2(a). The evaluation of the experimentally observed step–step distance (or equivalently the terrace width) provides a Gaussian distribution with an average of 2.04 nm and a standard deviation of 0.29 nm [17]. This corresponds to terraces in which 8 atomic rows parallel to the step edge are exposed with a deviation of ± 1.2 rows. The misorientation of the step direction is found to be small and the kink density is extremely low. These properties are not only found locally by STM but are also observed in He scattering from areas of the order of 1 mm^2. It was suggested that vicinal surfaces are stable only at high temperature as the entropic contribution of step vibrations provides a

substantial contribution in the balance of the free energy [18]. At high temperatures, where the samples are annealed during preparation, the minimization of the free energy favours the ordered vicinal surface with respect to facets, and at low temperatures, where facets become more favourable, the kinetics of reordering is too slow to allow a transition back to a faceted morphology. It has also been established that entropy plays an important role for the regularity of the step arrangement.

Entropy provides a mechanism for step–step repulsion, which leads to the regular step arrangement, however, with a broad distance distribution [15]. In the case of Pt(997) it has been shown in experiment [17] that the terrace width distribution is significantly narrowed with respect to pure entropic repulsion. This result directly indicates the presence of an additional repulsive interaction between the steps, which may arise due to lattice distortions or dipole–dipole interactions originating at the step edges. This ordering mechanism due to repulsive interaction has also been observed for other surfaces. Vanishing interaction or even weak attraction was found for the missing row reconstructed Pt(110) surface [19]. Detailed investigation of the dynamics of step edges can yield valuable information on the relevant step energetics [20].

For some vicinal surfaces, at high temperature entropy can lead to a destruction of step ordering in a roughening transition [21]. The transition occurs at the temperature where the free energy required to create a step vanishes and the step length can increase spontaneously. A practical consequence of this transition for the preparation of ordered vicinal surfaces is that after annealing to temperatures comparable to or above the roughening temperature the surface must be cooled down slowly in order to avoid freezing of the roughened morphology. An early calculation of the roughening transition for the vicinal Pt(331) surface, which is similar to Pt(997) but with terraces three rows wide, gave a roughening temperature of 570 K [22]. The values for vicinal surfaces with a larger terrace would be expected to be even smaller. This predicted onset may appear rather low, given the experimental value for the roughening temperature for Pt(110) being as high as 1080 K [23]. In fact, non-grazing He scattering shows no deviation from a Debye–Waller behaviour of the third-order diffraction peak between 300 and 750 K [24].

3. The fabrication of monatomic rows and superlattices and their properties

Vicinal surfaces exhibit functional centres, which are determined by the type and distribution of their steps. These centres can be modified in a straightforward way by adsorption of atoms or molecules. Given the importance of adsorption sites near step edges for growth and chemical surface reactions, surface properties of vicinal surfaces can be controlled efficiently without the necessity to cover the entire exposed surface. In order to modify the properties of vicinal surfaces in a controllable way one has to investigate the formation of adsorbate structures near the step edges and, specifically, step decoration.

The processes involved in decorating steps represent a subset of the processes playing a role in thin film growth. One can look at step decoration from two different sides: first, step decoration is the dominating process during thin film growth in between island nucleation and monolayer (ML) completion. Second, step decoration is the one-dimensional equivalent to epitaxy, i.e. layer growth. Of major importance are the kinetics of processes at step edges and exchange processes at steps for heteroepitaxial systems. These processes are presently under intense study by both theory and experiment. Apart from understanding the elementary processes during step decoration there is certainly much interest in the grown structures themselves. The study of the properties of one-dimensional adsorbate structures with respect to their electronic and magnetic properties is a field that is just emerging.

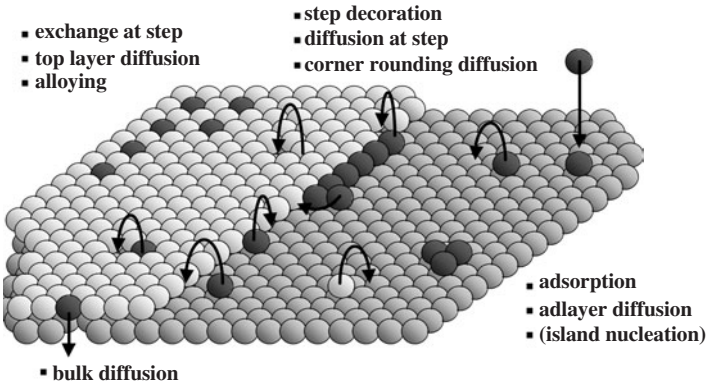

Figure 4. Surface processes relevant for growth on vicinal surfaces.

3.1. Processes involved in monatomic row formation at step edges

In the following we will restrict ourselves to the adsorption of metals on vicinal surfaces. The processes taking place during and after deposition of metal atoms are essentially the diffusion processes illustrated in figure 4. Molecular adsorbates may in general show a more complicated behaviour including dissociation, reaction, and desorption.

It is well known for the processes in thin film growth that there exists for a given adsorbate–substrate system a hierarchy of adsorption sites with specific binding energies. In thermodynamic equilibrium these sites become successively filled with increasing adsorbate coverage. On the other hand there is a hierarchy of diffusion processes which enable the system to reach equilibrium but which become active only above certain temperatures. These processes have been studied in detail; see, for example, [25–27]. Here, we will focus on the ones relevant for step decoration. In contrast to theoretical approaches describing growth in the long term and high coverage limit we will focus here on growth in the low coverage regime. Typical coverages correspond to the density of step atoms on the Pt(997) surface, which will be at the centre of our discussion. The coverages will typically be of the order of 10% of a ML.

Atoms deposited for example on a close-packed Pt(111) surface impinge on the terrace and bind initially to sites with a low coordination to 3 (or less) adjacent substrate atoms. The lower edge of a substrate step provides adsorption sites with higher binding energy than the terrace due to the increased coordination of the adatom. At the step the coordination of the adatom can increase to 5 at a straight step or 6 next to substrate kink sites (see also figure 4). We note that for metal adsorbates it is a valid first-order approach to correlate the binding energy of an adsorption site with the number of nearest neighbours. We add for completeness that as an exception to the rule, in certain systems with more complicated interactions the preferential adsorption site for an adsorbate is not at the high coordination site at the bottom but at the top of the step, like for O_2/Pt(997) [28] and Fe/Cu(111) [29].

There exists a thermodynamic equilibrium between atoms decorating the step and those diffusing on the terrace even under vanishing deposition flux. The high binding energy of adsorbates at sites at step edges has been well known for a long time from thermal desorption spectroscopy (TDS) of gases. If low adsorbate coverages on the terrace can be monitored, the additional binding energy at step sites can be obtained experimentally from the temperature dependence of terrace coverage [30]. For metal adsorbates, however, the temperature required for detachment from the step edge is too high to allow such a direct observation of this equilibrium. This indicates the strong tendency for step decoration in such systems.

An adsorbate on a low-index terrace can diffuse relatively easily on the flat surface. The activation barrier is lowest for close-packed terraces, which makes them well suited to obtain step decoration. During diffusion the adsorbate may either encounter other adsorbate atoms and aggregate to form a cluster or it may encounter a step edge. If the first process leads to an efficient immobilization of the diffusing atoms, which can, for example, already occur for a cluster of two atoms [25], then the branching ratio between these two processes determines the balance between island growth and step decoration [31]. Generally, island growth will become important at low temperatures (reduced terrace diffusion), large terrace sizes (increased time to encounter other atoms), and high adsorption rates (increased adatom density on the terraces). Only if all these contributions can be neglected do we have a situation in which almost every deposited adatom will attach to the substrate step, and step decoration is the dominating process.

High coordination sites at the lower step edge may become occupied by adsorbates approaching from both the upper and the lower terrace. The presence of an Ehrlich–Schwöbel (ES) barrier, however, often reduces the attachment from the upper terrace substantially. This barrier is defined as the activation energy of diffusion across a descending step minus the energy barrier for diffusion on an infinite terrace. It is a positive energy barrier when the involved adatoms pass through a transition state with reduced coordination. As a result, for many adsorbate/substrate systems the upper step edge is repulsive and efficiently reflects diffusing adatoms. Then, step decoration can take place exclusively from the lower terrace.

An adsorbate reaching a step will at low temperature irreversibly attach to it, but the atom may still be free to diffuse along the step edge. The site with the next highest binding energy is a site close to an atom in a kink position, which may efficiently immobilize the adsorbate. The encountered kink site will, for initial growth, belong to the substrate, but it will soon be a part of a growing one-dimensional adsorbate island at the step edge. The difference is of importance for heteroepitaxy where substrate and adsorbate atoms are subject to different binding energies and diffusion barriers. In heteroepitaxy the exchange between adsorbate and substrate atoms is an additional issue if one wants to generate defined structures.

Let us now focus on the growth after adsorbates have already attached to the step edge. If an adsorbate attaches in a region already covered by one row of adsorbates but the previous row has not been completed it becomes of importance whether the atom can be integrated into the previous row or it remains in the row where it first attached. The process necessary to reach the previous row is a corner-rounding process. Its activation energy determines whether the step edge advances as a straight line or starts to roughen.

In a step-flow growth mode the step edge advances without developing a significant defect concentration. A step adjacent to a terrace, which is wider than the average terrace width, is subject to an increased rate of adsorbate attachment. It will advance with a higher velocity than the average step edge if it is supplied only by attachment from the lower terrace. The mechanism obviously tends to stabilize the growth process and may result in an increased regularity of step–step distances.

If, in contrast, the step edge starts to roughen during growth (e.g. because of non-active corner rounding), the protruding parts of the step can capture more of the deposited adatoms than the recessed parts and the roughness of the step can increase even further. This results in a dendritic or fractal growth [32, 33] and may also be regarded as an extreme case of the Bales–Zangwill instability [34]. It also depends on an asymmetry of attachment from the upper or the lower terrace. There is, however, a factor counteracting the instability. Step roughening (on an atomic length scale rather than for a 'wavy' morphology) can reduce the ES barrier due to the increased number of kinks and allows more adatoms from the upper terrace to attach to a step. Theoretical studies of self-diffusion across Pt(111) steps [35, 36] show that the ES barrier for an exchange with a step edge atom is significantly lower than for a jump over the

step edge. The ES barrier is reduced even more by the presence of kink sites and may then even become negative. A similar result is found for embedded atom calculations for Ni adatoms crossing Pt(111) steps [36].

In conclusion, we find that perfect step decoration can be obtained if the potential energy of an adatom at the step edge is significantly lower than on the terrace (significantly here means with respect to the energy $k_B T$ in which T is the surface temperature) and the temperature is high enough that the essential diffusion processes (terrace diffusion, step diffusion, corner rounding) are active. This means that step decoration occurs at temperatures just high enough to establish the state with the lowest energy for the adsorbate. However, we have to be more precise in this statement with respect to heteroepitaxy: the obtainment of a pure adsorbate structure at the step edge requires that alloying processes be kinetically hindered because in heteroepitaxy systems the alloy might, indeed, be the state of lowest (free) energy.

3.2. Platinum homoepitaxy

Before we focus on heteroepitactic step decoration, the main subject of this article, we want to briefly discuss a system where step decoration can be studied in its pure form without accounting for the possible influence of alloying. In this section we compare the growth of Pt on Pt(111) and Pt(997) surfaces. The essential difference between the two surfaces is their average step–step distance, which is of the order of 100 nm on well prepared Pt(111) and 2 nm for Pt(997). Pt adatoms are mobile on the close-packed Pt terraces down to around 80 K [37, 38]. A fundamental study of Pt epitaxy on Pt(111) was presented by Kunkel *et al* [39]. They observed continuous oscillations of the specularly reflected He intensity at high temperature (621 K), which demonstrated the layer-by-layer growth mode. The fact that oscillations are observed suggests in addition that no step-flow mode occurs in which all deposited atoms are attached to pre-existing step edges and which would result in a constant reflected intensity. Instead, islands nucleate on the large terraces and coalesce to form a complete layer before the next layer starts to grow. When the surface temperature is reduced to 424 K, the He intensity oscillations disappear and change to an exponential intensity decay which indicates the development of a rough morphology in which the number of exposed layers continuously grows. In a third regime at still lower temperature (275 K), the oscillations reappear, for which the expression re-entrant layer growth was coined. The reappearance of oscillations at low temperature is due to the strongly reduced island size leading to a reduced ES barrier for interlayer transport.

We now want to contrast these results with the measurement of Pt deposition on Pt(997) in which, as said before, the essential difference is the average terrace width. Figure 5 shows the *in situ* He reflectivity during Pt deposition, which begins at time zero on the annealed Pt(997) substrate. The measurement is done in grazing angle scattering geometry, which will be used in the following sections to monitor step decoration. This geometry is specifically sensitive to the presence of kink sites and to the morphology at the step edges during the growth process. For more details see [13]. From the discussion on crystal planes of vicinal surfaces in section 2 it is clear that we cannot expect oscillations originating from layer-by-layer growth unless we create islands on the 2 nm wide terraces. For the employed evaporation rate (of the order of 10^{-3} ML s^{-1}) this is, in fact, not the case even below 130 K, as the adatom remain sufficiently mobile. We may rather expect to observe oscillations for the completion of successive crystallographic layers, i.e. rows attached to the steps. However, there is no temperature at which oscillations can be observed. Instead, we find a transition from a continuous increase of kink density (at low temperature) to a mode where the kink density stays constant (at high temperature). In analogy to step-flow growth we can call this situation kink-flow growth. The data show that the defect density increases at a rate which

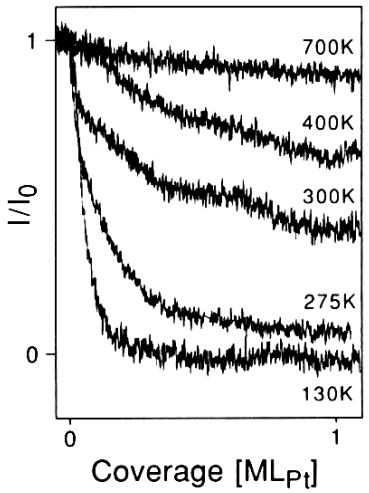

Figure 5. Specularly reflected He intensity in grazing scattering geometry during *in situ* Pt deposition on Pt(997) at different temperatures. He diffraction order: $n = 0$. Incidence angle of the He beam with respect to the surface normal: $\theta_i = 80.0°$; angle of He detection with respect to the surface normal: $\theta_f = 80.0°$; from [13].

becomes smaller with increasing surface temperature. The initial slope, however, assumes essentially two values: a small negative slope above 400 K and a steep negative slope below 300 K. Between these temperatures the formation of separated short Pt chains at the step edges sets in. Below 300 K no kink density oscillations occur, which suggests that atoms attaching at these chains in the second row cannot complete the monatomic chains. At 300 K the corner-rounding process must already be frozen in. In fact, theoretical studies suggest that diffusion along step edges and corner rounding become deactivated at approximately the same temperature: the relevant corner-rounding barrier ($\approx$0.74 eV) is close to the barrier for diffusion along the step edge (0.77 eV) (B-type step for Pt(997)) [40]. Both barriers are substantially higher than the terrace diffusion barrier of 0.26 eV [41, 42] or 0.33 eV [43], which explains the onset of step roughening at 300 K.

As mentioned earlier, calculations have shown that self-diffusion across step edges is most efficient by means of atom exchange next to kink sites. For this process the ES diffusion barrier remains only slightly larger than the diffusion barrier on the terrace [35]. On a well annealed surface with low kink concentration the density of kink sites is low, and the effective barrier of exchange over straight B steps will be close to the straight-step value of 0.4 eV [35], leading to an efficient reflection at the step edge. When the step roughens during growth one can expect that adatoms can more easily overcome the barrier for step-down diffusion. Atoms adsorbing on the upper terrace will then increasingly supply the advancing step edge. As this in turn results in a reduction of step roughness a temperature-dependent equilibrium will eventually establish. The data in figure 5 support such a behaviour.

The comparison between homoepitaxial growth on Pt(111) and Pt(997) demonstrates the different processes dominating growth on the two surfaces. Pt(111) forms a flat two-dimensional substrate on which growth is dominated by island nucleation on large terraces and the transfer rate of adatoms between different layers. For Pt(997), terrace diffusion can be regarded as fast for temperatures above 80 K. The reason is the small distance between the adsorption site of the evaporated atom and the nearest step. On Pt(997) it takes an adsorbed atom on average only 52 hops (elementary diffusion steps) to reach an ascending step if we

assume the descending step to be repelling and all hops to be equivalent (i.e. having the same barrier). The growth mode on Pt(997) is determined by the formation of separate pieces of Pt chains at the step edge and by the transfer between adjacent adsorbate rows attached to the step edge. The relevant processes on Pt(997) thus occur in a dimension reduced by one with respect to the processes on Pt(111), while the transfer across steps also plays a role on Pt(997). We finally note that in figure 5 the slope at the start of deposition is negative for all temperatures. This means that the Pt(997) steps cannot be made any 'smoother' by Pt deposition than they are made by annealing during the preparation.

3.3. Heteroepitaxy in step decoration

The systems which are of more interest from the application point of view than the system we discussed above are, certainly, heteroepitaxial systems, which will be the subject of this section. In order to obtain step decoration in a heteroepitactic system the growth temperature possesses a strict upper limit: the onset of alloying between adsorbate and substrate can destroy elementally pure row structures at the step edges. This requirement and the prerequisites for step decoration can be fulfilled at the same time if alloying becomes active at higher temperatures than the diffusion processes needed for ideal step decoration. Usually, alloying plays a role only at increased temperature as the alloying process requires the generation of a sufficiently high coverage of vacancies in the terrace (surface alloying) [45] or in the bulk (bulk alloying), which is connected with a substantial energy cost. There are, however, cases where this is not the case, for example Ni/Pt(997) where exchange processes at the step edge are observed already at 150 K [44]. Ni was found to exchange with a step atom while descending a step on Pt(111) with a very low ES barrier (0.08 eV) [36].

The experimental access to monitoring step decoration *in situ* has already been sketched in section 3.2. Thermal energy He scattering is a diffraction method which will be applied in the following to analyse the initial growth of various metals on Pt(997) and Pt(779). In grazing scattering geometry the method allows us to monitor changes of the defect density at the step edges during the evaporation of metals from an electron beam evaporator at a fixed deposition rate of the order of 10^{-3} ML s^{-1}. The rate is calibrated by the observation of ML oscillations at non-grazing scattering geometry. Figure 6 shows several sets of He reflectivity curves monitored during the deposition of different elements and at a series of substrate temperatures. Let us start the discussion of the observed features by focusing on the $T = 300$ K measurement of Ag deposition. At the beginning of deposition the reflected He intensity decreases due to the creation of defects at the substrate step edge which becomes decorated by the adsorbate. After passing through a minimum the intensity rises again and reaches a sharp peak at a coverage of about $1/8$ of a ML. This peak corresponds to a low defect density and can be ascribed to the completion of a monatomic row of Ag attached to the lower step edge in agreement with the known substrate step density. At a coverage of $2/8$ ML a shoulder is observed which reflects the completion of a second Ag row attached to the step edge. During further deposition no further sharp reflectivity peak is observable. Only a broad structure appears with a maximum near 0.5 ML coverage. This maximum reflects a continuing growth with a comparatively low defect density. Figures 3(b), (c) show STM images of Ag step decoration at 340 K. Figure 3(b) demonstrates that at coverages below the substrate step density short separated Ag chains are formed which appear as protrusions at the straight substrate step. For a coverage of 0.14 ML an almost perfect step decoration by a monatomic row of Ag is obtained (figure 3(c)).

The reflectivity peak at $1/8$ ML results from step decoration due to the higher binding energy at the step edge. The diffusion barrier of Ag on the Pt(111)-type terrace is 0.17 eV [46, 47] and thus substantially lower than for Pt self-diffusion. The binding energy

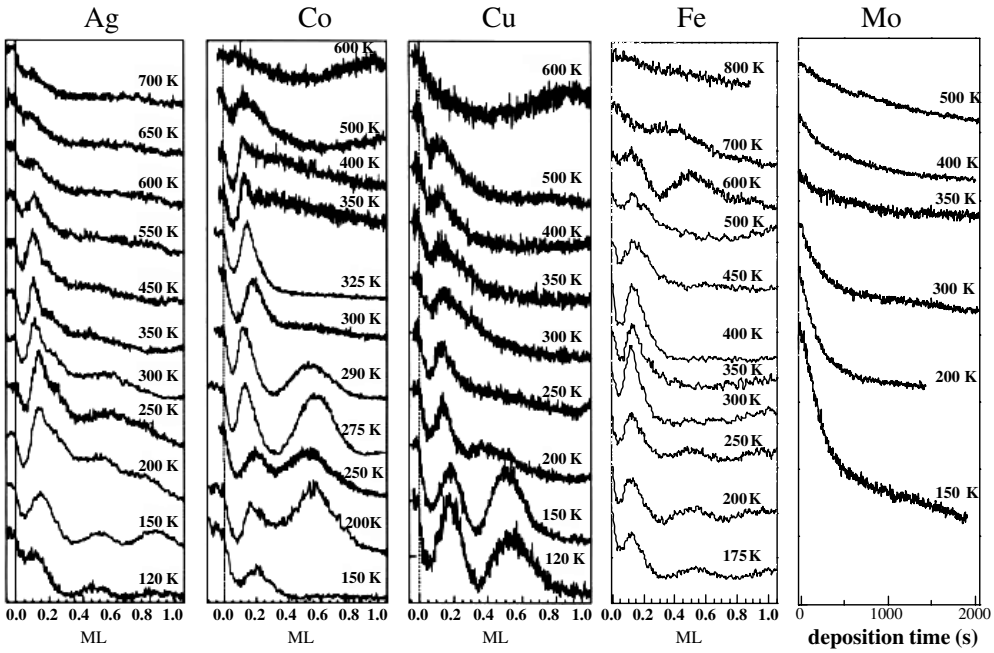

Figure 6. He grazing angle specular reflectivity (diffraction order $n = 0$) during monolayer deposition of the elements Ag, Co, Cu, Fe, Mo as a function of temperature.

of Ag in the first and second row at the Pt(997) step edge was calculated by semi-empirical potentials to be with respect to vacuum potential -3.15 and -2.80 eV, respectively [48]. The binding energy of Ag to the Pt substrate step is thus 0.35 eV higher than to a step edge pre-covered by a row of Ag. This situation is also found for the adsorbates Cu and Co [48] and indicates the specific property of the substrate with respect to its interaction with these adsorbates. The calculation explains the stability and the wide temperature range found for step decoration on Pt(997) evident from figure 6.

As pointed out earlier, alloying is an important issue if one wants to generate elementally pure rows of monatomic width at the step edge. The measurements show that even at the surface or bulk alloying temperature step decoration can be observed. This indicates that a Pt step edge decorated by one adsorbate row represents a very stable arrangement. It also suggests that alloying occurs not through the terrace but predominantly at the step edge. If the terrace would allow efficient alloying the adsorbates would not reach the step to decorate it and the coverage necessary to obtain a monatomic row would increase with temperature, which is not observed. Step decoration may in principle promote alloying due to the increase in the number of attempts which the adsorbate can make to exchange with the substrate. In addition, exchange at the step edge may require a lower activation energy due to the lower coordination of nearby substrate atoms.

The height of the first peak in the deposition experiments in figure 6 is an inverse measure of the minimum defect density averaged over the observed surface area at the coverage at which the first row is completed. It can be qualitatively evaluated using the fact that a higher intensity corresponds to a better order of the structure. However, different metals exhibit different reflectivities. Ag, for example, has a specifically intense first-row peak, which may be correlated with the observation that a complete Ag ML has a higher reflectivity (in non-grazing scattering geometry) than the clean Pt substrate. The low intensity of the peak related

to the completion of the second row might indicate an increased defect (kink) density in this row. It would corroborate the reduction binding energy in the second row, mentioned above. However, another phenomenon has to be taken into account. We already discussed that the statistical distribution of terrace widths can be described by a Gaussian with a standard deviation of approximately one row (0.29 nm). A terrace with a larger width collects more deposited atoms than a terrace with smaller width. The velocity at which straight step edges advance depends on the width of the nearest (lower) terrace. This results in a desynchronization of row completion on different terraces and thus in a smearing-out of the observed row oscillations. A simple statistical model is already sufficient to account for the reduced second-row peak height and a completely damped-out third peak if a realistic terrace width distribution is assumed. The straightforward calculation and the result are presented in the appendix of this article. In the simplest model the growth rate of a given step is determined only by the initial width of the adjacent terrace. The rate is assumed to stay constant and independent of coverage. The simulations shows an interesting feature: in the case when the diffusion barrier is kept at a spatially fixed position a re-synchronization of the oscillations is expected with peaks at coverages of $6/8$ and $7/8$ MLs, which corresponds to, respectively, 2 and 1 rows missing to ML completion. In contrast, no such re-synchronization is obtained, if coupling of regions with slightly different terrace width (modelled by non-integer terrace widths) is allowed or the diffusion barrier is attached to the advancing step. The fact that for none of the metal adsorbate systems studied re-synchronization of the oscillations was observed might thus suggest that the advancing step and not the immobile substrate–adsorbate frontier forms the diffusion barrier or the effective barrier height changes during growth. There are, however, results supporting a pinning of the diffusion barrier: for Ag growth on Pt(111) the ES barrier across an Ag step edge was experimentally determined to be as low as 30 meV [49]. Also for Ag/Pt(997) the advancing step edge may no more be an efficient diffusion barrier. Moreover, the barrier blocking the diffusion perpendicular to the steps may become located inside a terrace at the boundary between Pt and Ag which is the position of the initial Pt step edge [49].

From the modelled decay of row oscillations one would assume that after the formation of the third row no further information on the growth could be obtained. In contrast, figure 6 shows that structures in the reflectivity curve can still be seen around 0.5 ML coverage. These peaks are a clear indication of growth with a low defect density. However, a complete interpretation of the reflectivity maxima cannot be given because the variation of reflectivity turns out to be determined by numerous contributions, which could not be separated experimentally. An interpretation only in terms of varying defect density is clearly too simplistic for higher coverages and is not supported by STM investigations under similar conditions.

The coverage at which the peak of the first row completion is observed shifts with substrate temperature. The peak position as a function of temperature is plotted for different adsorbates in figure 7. At low temperature the defect density reaches its minimum when the amount of deposited atoms exceeds by 50% the coverage required to decorate the step edge. A strain-induced structural transition at the step is unlikely to account for this observation. The percentage of lattice mismatch is much smaller than the observed peak shift, which in addition is always towards higher coverages. The lattice mismatch for Ag (+4.3%) has the opposite sign of mismatch to Cu (-7.9%) and Co (-9.7%). The mismatch is calculated for nearest neighbour distances in the bulk of the adsorbate with respect to bulk Pt. Due to the small mismatch the adsorbates grow in the first ML pseudomorphically. The shift in coverage of the first peak can be attributed to a trapping of the adsorbates in the second or higher row, which results in a delayed minimization of the kink density. The STM image of Ag deposited at 120 K (figure 3(d)) corroborates this interpretation: there is no longer a complete wetting of the substrate step by Ag. The data in figure 7 show that the underlying deactivation of corner

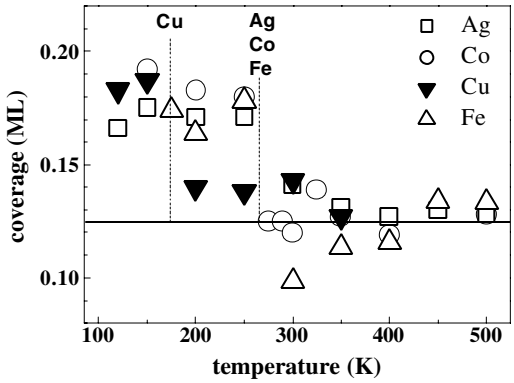

Figure 7. Adsorbate coverage at the position of the first-row reflectivity peak in grazing He scattering as a function of temperature for the elements Ag, Co, Cu, and Fe.

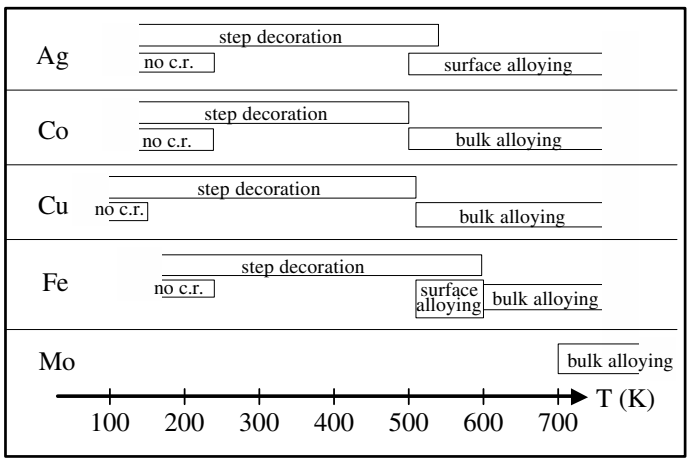

Figure 8. Overview of the growth behaviour of different elements on Pt(997) in the sub-ML range; 'no c.r.' = corner rounding not active.

rounding occurs for Cu at around 175 K, and for Ag, Co, and Fe at around 250 K. These temperatures define the lower limit for the formation of perfectly monatomic chains at the step edge. Kinetic Monte Carlo simulations based on semi-empirical potentials have confirmed that for the Ag/Pt(997) system the completion of the first row is delayed at low temperature for the employed adsorbate flux around 10^{-3} ML s^{-1} [50]. Much stronger shifts are predicted to occur for the system at an adsorbate flux above 1 ML s^{-1} for temperatures below 200 K.

Having introduced and discussed the essential mechanisms for the example of Ag in detail, we give a summary of the behaviour of the adsorbates Ag, Cu, Co, Fe, and Mo in figure 8. A few additional remarks shall be added with respect to Co, Fe, and Mo.

In an STM study Co was found to form at the step edge islands of more than monatomic height in the temperature range 300–500 K and at coverages of a few rows [51]. In the He reflectivity data (figure 6) this growth mode can be identified by the absence of He reflectivity around 0.5 ML coverage and the slow reflectivity decrease after single-row completion. In this temperature range monatomic chains are still created with a defined geometry. Co stripes developing after row completion, however, are no more restricted to monatomic height.

Fe exhibits surface-restricted alloying which sets in between 450 and 500 K. This is concluded from a substantial shift in the He reflectivity oscillations in the 1–2 ML range [52]. The peak for monatomic step decoration in figure 6 is still present at 600 K, which indicates that Fe still decorates the step edge even above the alloying temperature. It is observed that alloying occurs under these conditions on a timescale of a few minutes, which is comparable to the deposition time of one row of Fe. The Fe row is thus stabilized at the step edge but can probably dissolve into the terrace.

Mo is the only of the adsorbates presented here which does not exhibit monatomic row formation. Figure 6 shows no reflectivity oscillations at any temperature, and the same applies for non-grazing scattering geometry (not shown here). As no oscillations due to layer completion are observed we have no means to reliably calibrate the coverage for this element. The coverage scale in the figure is replaced by the deposition time. A small shoulder observed in non-grazing He scattering might suggest that ML coverage is reached at a deposition time of 750 s. At first glance the case of Mo might appear similar to Pt homoepitaxy. Also the lattice mismatch of Mo on Pt is only -1.4%. However, for Mo the initial slope remains steep up to 600 K and there is no indication for kink-flow growth. The deposition most likely provides a rough surface morphology throughout the temperature range studied, 150–600 K. From Auger spectroscopy we find that bulk diffusion of Mo occurs only above 700 K in agreement with results by Bassett [53]. As the behaviour remains similar throughout the studied range a high diffusion barrier may well explain the results.

The experimental observations of the different adsorbates (figure 6) can be correlated to data on surface alloying provided by Christensen *et al* [54] based on density-functional calculations and on effective medium theory. According to these calculations Ag is the only element discussed here which exhibits surface segregation on bulk Pt; the others show no segregation. The experiment demonstrates, however, that stable rows at the substrate steps are formed for Co, Cu, and Fe. Mo has a tendency to mix with the Pt substrate (mixing energy 1.98 eV/atom) and also a strong tendency for antisegration, which can explain the missing of step decoration at least at high temperatures.

At the end of this section we want to come back to the role of the step microfacet for the properties of a vicinal surface and make a comparison between Pt(997) and Pt(779) surfaces. From figure 2 it is clear that there is neither a difference in step height nor in the coordination of step sites for the two surfaces. We can thus expect that many properties will be similar. No significant difference is indeed found for the behaviour of step reactivity for O_2 dissociation [28] as this process does not occur at the immediate step edge. No substantial difference was found for Ag step decoration [24] although the microfacet of the step plays a role for the details of interlayer diffusion, diffusion along the step edge, etc and one might expect minor changes in the growth modes and the onset temperatures for processes at the step edge.

A significant difference between the two vicinal surfaces with the different step-types was, however, found for alloying of Ag with the Pt substrate. Above 620 K, Ag forms a surface-restricted alloy on Pt(111) in which Ag forms patches inside the Pt(111) terraces [55]. Above 600 K the alloy can be formed on both Pt(997) and Pt(779) [24]. When Ag is deposited above alloying temperature the alloy forms but starts to become overgrown by the advancing step edge which leads to demixing as the alloy is not stable in the buried layer. At ML coverage the equilibrium is established with a pure ML of Ag covering the substrate. Reaching ML coverage this demixing is manifested in non-grazing geometry He scattering by a sharp rise of He reflectivity. It can be ascribed to a fast removal of compositional disorder. Figure 9 shows a comparison of the temperature dependence for Pt(997) and Pt(779). The shape of the *in situ* reflectivity curves is similar for the two surfaces. The demixing feature near ML coverage appears at high temperature as a large peak, at lower temperature as a shoulder. At 400 K

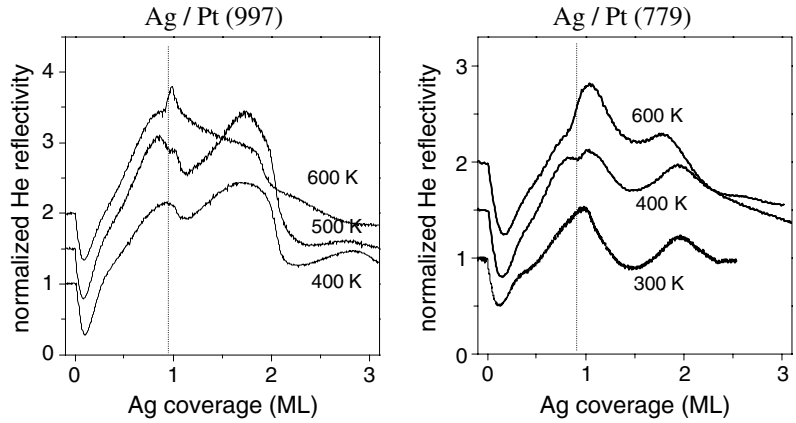

Figure 9. Ag demixing features on Pt(779) and Pt(997). The He reflectivity in non-grazing scattering geometry is plotted as a function of Ag coverage for a set of temperatures covering the onset of demixing. The onset temperature is about 400 K on Pt(779) and 500 K on Pt(997). Diffraction order $n = -2$.

the feature starts to appear on Pt(779) while it is still absent on Pt(997) and only appears at 500 K. This temperature difference is substantially larger than a possible error in temperature measurement. We can assume that the free energy of the alloy on the close-packed terraces does not differ for the two surfaces. The different onset of alloying thus demonstrates that the microscopic step structure plays an important role either for the energy balance of the alloyed phase or, more likely, for the kinetics of its formation.

In summary, the elements Ag, Cu, Co, and Fe decorate the Pt(997) steps over a wide temperature range (at least 200–500 K). The decoration is still observable as a small peak or shoulder at temperatures where surface or bulk alloying occurs. The low-temperature limit where no coherent monatomic rows are formed is around 175 K for Cu and around 250 K for Ag, Co, and Fe. Mo does not exhibit row formation at the substrate step edge in the range 150–500 K, probably due to reduced diffusion.

3.4. Growth and stability of superlattices

The creation of one-dimensional structures can go beyond the preparation of monoelemental chains with a width of one atom to a few atoms. In fact, the step structure after adsorption of one element can be used again as a template for the adsorption of a second element. This allows assembling one-dimensional sandwich structures. The structure can be regarded as a deliberately assembled ordered alloy with the advantage that it does not have to represent an equilibrium structure but may only be metastable. We will see that the creation of a metastable sandwich puts even more emphasis on the question of spontaneous alloying at step edges. The elements deposited in the experiments which we discuss below exhibit a strong tendency to alloy with each other or with the substrate. Only Ag behaves mostly like a step-edge surfactant, but forms a surface alloy at higher temperature as was already discussed in section 3.3. The functionality obtainable by sandwich structures is due to the fact that they provide a defined spatial distribution of various binding sites, e.g. for the adsorption of gases. The catalytic activity of a surface depends on the detailed shape and atomic composition (including all neighbours) of such sites.

In order to address the formation of sandwich structures of metals on Pt(997) two studies will be discussed which monitor the growth of these structures again by *in situ* He scattering

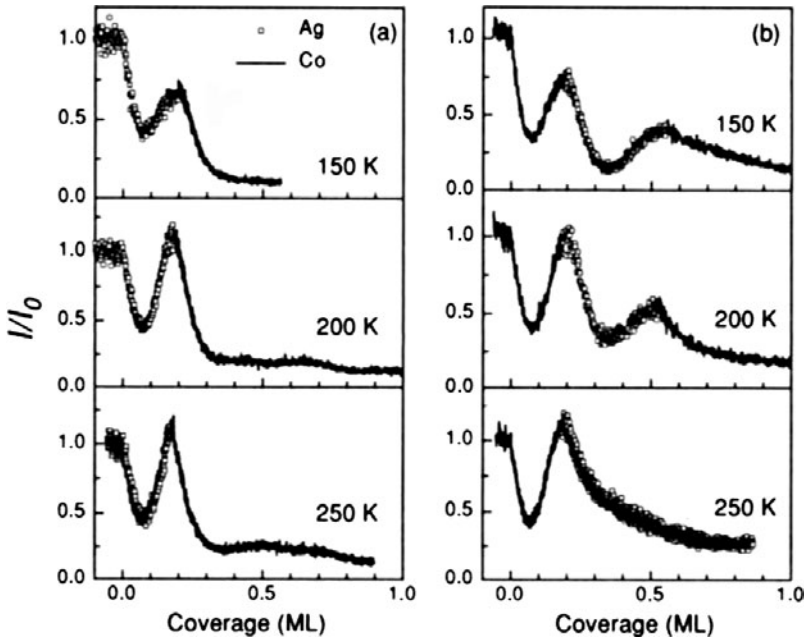

Figure 10. He specular reflectivity in grazing geometry during deposition of Ag + Co sandwich structures on Pt(997) for different temperatures: (a) Ag row formation followed by Co deposition; (b) Co row formation followed by Ag deposition. He diffraction order $n = 0$; $\theta_i = \theta_f = 83.0°$).

in grazing scattering geometry. As discussed in section 3.3, the formation of a second row is not always clearly detectable even when the growth proceeds without substantial roughening. However, reflectivity maxima appearing in the sub-ML range can be taken as a strong indication that structures with low kink density prevail. A reflectivity at grazing incidence which is comparable to the one of the freshly prepared substrate is incompatible with a rough step edge for an otherwise similar surface morphology.

Two sandwich systems, Ag + Co and Ag + Cu, will be discussed. The attachment of the elements at the Pt(997) step edge is monitored in both deposition orders and at various temperatures as shown in the figures 10 and 11. As discussed in section 3.3 row completion followed by a growth with low kink density are observable for Ag, Co, and Cu. In order to obtain the sandwich structures the deposition of the first element is stopped on the peak of first row completion. After a delay of a few seconds, during which the reflectivity remains constant, the second element is deposited.

The deposition of Co after Ag pre-deposition is shown in figure 10(a). A strong decrease of reflectivity is observed. In contrast, Ag deposition on a surface with Co covered steps (figure 10(b)) leads to a high reflectivity near 0.5 ML total coverage [48]. This demonstrates first of all that the order in which Ag and Co are deposited is relevant and two different surface morphologies are created. It also suggests that Ag decoration of a Co pre-covered step proceeds similarly to Ag decoration on the clean Pt(997) (see figure 6). This does not hold for the reversed deposition order. He scattering has some implicit chemical selectivity due to its high sensitivity to atomic surface corrugation. Thus the low reflectivity can either be due to atomic exchange at the step edge or a strongly increased kink density. As the pure metals exhibit a growth mode with high reflectivity at low temperature, both effects would indicate the occurrence of alloying. Intuitively, the alloying of Ag and Co at the step edge may appear

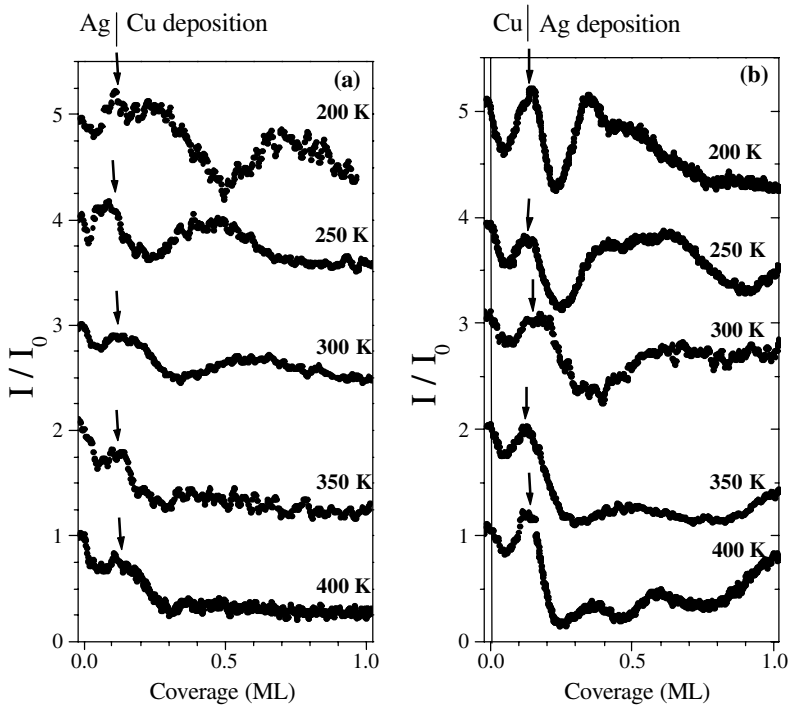

Figure 11. As figure 10 but for Ag + Cu sandwich structures: (a) Ag row formation followed by Cu deposition; (b) Cu row formation followed by Ag deposition. He diffraction order $n = 0$; $\theta_i = \theta_f = 85.0°$).

favourable because of the opposite sign of the lattice mismatch of the two elements on Pt(111). The result suggests, however, that a basically element-separated structure is obtained if Co is deposited before Ag deposition between 150 and 200 K.

One may draw an analogy between the deposition of sandwich rows of Ag + Co and sandwich MLs on Pt(997) which is discussed in more detail in [48]: deposition of Co multilayers on Pt(997) pre-covered by an Ag ML shows a rapid decay of He reflectivity with coverage (in non-grazing scattering geometry) whereas Ag on Pt(997) pre-covered by a Co ML exhibits reflectivity oscillations which can be ascribed to a continued layer-by-layer growth. Here, the surface free energies of the elements and their interface energies suggest that a sandwich of MLs of the form Ag/Co/Pt(997) is energetically favoured. With all the caution necessary in generalizing this result one might take the observation as an indication that elements with the lowest surface free energy (here Ag), which tend to form a stable surface layer, also tend to form a stable capping of the step edge.

The measurements of *in situ* deposition of the second sandwich system, Ag + Cu, are displayed in figure 11. It is obvious from first inspection that at lower temperature both deposition orders lead to structures with high reflectivity during the growth of the first ML. In contrast to the Ag + Co sandwiches here both deposition orders lead to structures with high reflectivity. The different positions of maxima in the measurements suggest that the details of surface morphology vary with deposition temperature. However, a full account of these features cannot yet be given. The temperature range for creation of an ordered structure covers 200 and 250 K. At 300 K the reflectivity is already lower, and it disappears around 350 K. The structural order, judged from the reflectivity normalized to the value of the Pt(997) substrate,

is high for the Ag/Cu/Pt(997) sandwich. Here, an intense and sharp second peak is observed close to the completion of a second Ag row (figure 11(b), top). This high reflectivity and a slightly larger temperature range of observation indicate a slightly higher stability of the Ag/Cu/Pt(997) sandwich with respect to the one created by the reverse deposition order.

The experimental results demonstrate that the Pt step edge decorated by one row of the elements Ag, Cu and Co does not form the same starting point as a well prepared clean Pt step edge. One reason is the different interaction potential of a pre-covered step with respect to the clean Pt substrate step. We already pointed out above, that the binding of Ag, Cu, and Co to the Pt step edge is specifically high [48]. Only step decoration by an adsorbate row with a similar property would allow observing a reflectivity peak corresponding to the first row of the second element. From the experimental point of view the sandwich system Ag/Cu/Pt(997) appears to be closest to this ideal situation.

We can obtain a first insight into the energetics of the sandwich system once more from calculations on surface alloys based on density-functional calculations and on effective medium theory [54]. Of the four elements only Ag tends to segregate from the bulk of the other elements. Ag does this on Co, Cu, and Pt. Cu impurities on an Ag bulk exhibit a small positive segregation energy (0.15 eV/atom), which may explain the occurrence of a metastable phase for Cu in contrast to Co. Only Ag shows a pronounced demixing on the Pt surface; all other elements show a tendency for mixing, and the system Cu on Pt shows the weakest tendency. Even though the calculations contain no information specific to the behaviour energetics at step edges the derived tendencies are compatible with the behaviour observed experimentally for the one-dimensional sandwich structures.

In a next step the experimental result can be discussed more adequately in the light of a theoretical calculation which was developed to model closely our experimental situation for finite temperature [48]. The calculations based on semi-empirical interaction potentials describing the Ag + Co and the Ag + Cu systems find a different thermodynamic behaviour for the two systems. Whereas the first sandwich system exhibits an absolute minimum in the free-energy map, which suggest stability only of the Ag/Co/Pt(997) sandwich, the second system develops apart from the Ag/Cu/Pt(997) minimum a second (local) minimum for Cu/Ag/Pt(997). This result suggests that for Ag + Co the driving force towards the stable arrangement is high, provoking mixing during Co deposition when Ag was pre-adsorbed. In contrast, the Cu/Ag/Pt(997) arrangement can form a metastable structure.

In the evaluation of the experiment we have to deal with the difficulty that He scattering has only an implicit chemical sensitivity but does not allow chemical analysis. We thus cannot directly access the chemical composition in the rows. The calculation predicts that at equilibrium none of the rows stays absolutely pure [54] but exhibits up to 20% of the second element (the mixing with Pt was excluded in the calculation). Detailed STM measurements may be able to access the composition at the step edge, at least for certain element combinations which provide sufficient height contrast.

The experimental aim to deposit the second element of the sandwich immediately after the deposition of the first element did not allow a choice of optimum deposition temperature for the first element. In this respect, further improvement of the deposition protocol and a better definition of the stripe may be achievable.

In summary, we find that the creation of sandwich structures at the step edge is feasible but is much more delicate than the decoration of the Pt(997) step edge by a single element. The reason is the importance of the driving force for the mixing of the adsorbates, which is found to play a minor role if only one metal is decorating the Pt(997) step edges. For the sandwich system the exchange processes at the step edge can be hindered by choosing a low surface temperature. However, this cannot guarantee that all element combinations can be realized because a

low temperature also deactivates other diffusion processes. Theory has proven successful in modelling the behaviour of the sandwich systems studied here. Similar theoretical analyses are thus very helpful in estimating the feasibility of creating more complicated structures. A coarse indication of the behaviour of sandwich systems might already be obtained from results (theoretical or experimental) of thin layer properties.

3.5. Properties of one-dimensional structures

One of the motivations for the generation of monatomic rows is the investigation of their physical and chemical properties. For several properties of interest, studies can already be found in the literature. Examples are the magnetic properties of monatomic rows and of small clusters with different shapes, the catalytic properties of the step edge region and the electronic states of monatomic rows. We briefly sketch these three subjects and refer to the literature for further reading.

The breaking of bulk symmetry at the surface has a significant impact on magnetic properties of ultra-thin films. The magnetic anisotropy is strongly affected and can switch as a function of layer thickness. Orbital magnetic moments, which are screened in the bulk crystal field, can make significant contributions in thin layers. The reduction of symmetry to one-dimensional structures will increase these effects even more, given the strong dependence of magnetic properties on coordination and interatomic distance. Within the Heisenberg model, however, no ferromagnetic behaviour is expected for a monatomic chain of atoms with magnetic moments. In practice, however, interactions of higher order and coupling to the substrate may lead to unexpected properties. Monatomic Co rows decorating the Pt(997) steps exhibit a superparamagnetic behaviour [56] with an easy magnetization axis pointing perpendicular to the step edge inclined towards the normal of the step microfacet. A remanent magnetization was found for the monatomic chain below 15 K. It is of interest to continue studies on similar systems in order to understand the underlying principles and coupling schemes. In this respect theoretical calculations are of increasing importance. They have a high predictive power and allow selecting systems of interest for experimental investigation. Theory has for example predicted that 4d elements, which are not ferromagnetic in the bulk, can also exhibit substantial magnetic moments in small clusters on a surface [57]. The size of these moments depends critically on element, cluster size and even cluster geometry.

The adsorption and reaction of gases at surfaces depends on the properties of specific adsorption sites, which often constitute only a small fraction of the catalyst surface. These sites obtain their specific properties from their morphology and by the chemical composition of the surrounding. The modification of step edges allows assembling specific sites with known geometry and composition. This has been demonstrated for a model system of site-induced dissociative adsorption of molecular oxygen on Pt(997) and Pt(779) [28]. The sticking probability of molecular oxygen from the gas phase decreases by an order of magnitude when the step edge is decorated by a monatomic row of Ag. Both vicinal surfaces exhibit a quantitatively similar behaviour. The dissociation site is found close to the preferential adsorption site of atomic oxygen at the upper step edge. Calculations identified the change in reactivity to be due to a change in precursor binding energy and not due to a change in dissociation barrier. The mechanism is thus different from the one for NO dissociation on Ru(0001) which takes place across the step edge [58] and which also can be expected to be substantially modified by step decoration.

The electronic properties of one-dimensional atomic arrangements have attracted much interest from photoemission studies of electronic band formation [59] to recent local STM studies on assembled Au rows [60]. Such studies can readily be extended to structures

assembled at step edges [61]. A future goal might be a direct investigation of conductivity in monatomic chains, which is, however, difficult to achieve for conducting or even semiconducting substrates. This motivates the development of preparational methods based on vicinal substrates, which allow obtaining one-dimensional metallic structures on insulating layers (e.g. [62]). Another approach to prepare low-dimensional electronic structures has been developed in recent years for the growth of quantum wells on GaAs substrates [63, 64].

3.6. Growth of layers on vicinal surfaces

There are only a few studies on the growth of multilayer films on vicinal surfaces. With respect to adlayer stress the formation of small adislands on terraces and islands attached to substrate step edges are not equivalent. A different growth behaviour can result from their different properties. As we discussed earlier, step decoration can under certain conditions completely suppress the formation of isolated adsorbate islands and force the growth of islands which are laterally attached to the substrate. This can happen even in cases where this morphology may be energetically unfavourable. With vicinal surfaces one thus has a means to force the formation of a flat first layer and reduce roughening at the early stage of growth. This behaviour is observed for example for Fe deposition on Pt(997): oscillations up to the second Fe adlayer are observed by non-grazing He scattering at 400 K [52] while three-dimensional growth (Vollmer–Weber growth) is reported on Pt(111) [65]. A similar difference is found for Cu growth on Pt(997) with respect to growth on Pt(111) [66, 67].

In contrast to forcing smooth layer growth in the ML coverage range, the growth at higher coverages may become even more irregular than on a low-index surface. On a stepped surface the lattice mismatch of adsorbates and substrate affects not only the ordering within the terrace plane but can lead to substantial stacking problems in the step region. Generally, layers can compensate partially for an epitaxial in-plane lattice mismatch by a modification of the layer height. If the adsorbate lattice is, for example, expanded with respect to the substrate the adsorbate layer will exhibit a smaller layer height than in the corresponding homoepitaxy case. At the step this behaviour will lead to an even larger height mismatch, so that restrictions for pseudomorphic adlayers (adlayers that adapt the lattice constant of the substrate) are expected to be much stronger than for low-index surfaces or vicinal surfaces with large step–step distances. We found by He reflectivity in non-grazing scattering geometry that oscillations due to layer-by-layer growth were strongly damped for most adsorbates. The oscillations continued for several MLs only at low temperature [24]. For Ag epitaxy on Pt(997), for example, more than five oscillation were observed at 200 K. Above 250 K only three oscillations are visible. At 400 K the oscillations disappear completely and surface facets appear in He diffraction scans. We expect that in such a case the multilayer film will at low temperature exhibit a morphology dominated by defect planes, which emerge from the former step edges [24]. However, we are not aware of detailed structural investigations of such a system. The periodic variation of strain and the presence of periodic defects may lead to unexpected thin film properties of such adlayers.

4. Outlook: kinked surfaces

In the experiments described in this article, monatomic rows were assembled at substrate steps. It was shown that these rows could be made tens of nanometres long with a length restriction given by the distance between substrate kinks. The kinks provide for the adsorbate a site with a coordination that is higher than for sites at the straight step edge. When diffusion along the step edges is active the kinks act as efficient nucleation sites for the growth of rows

at the steps. This favours a kink-flow growth mode. The control of kink density and kink arrangement allows us therefore to introduce another parameter determining the construction of new surface structures. It may allow obtaining chains with defined length and position. It may also allow assembling structures at a high density almost in an atom-by-atom fashion and in a highly parallel process. A complex surface structure with a periodicity defined by the initial kink period may thus be assembled by depositing subsequently sub-ML amounts of different adsorbates. The first requirement for this experiment is a stable, regularly kinked surface, which is an (hkl) surface with h, k, and l all different from one another (this is a necessary, not sufficient, condition). The surface normal then lies outside the azimuthal plane chosen in figure 1. Such kinked surfaces have been employed as surfaces with chiral centres [68].

There are still many questions arising with respect to such experiments. These 'kinked' surfaces are to some degree equivalent to the stepped ones discussed above but at a still lower dimensionality. Under which conditions and for which elements can such surfaces be prepared without kink bunching? Do kinks with the same geometry repel each other so that an ordered array with only small deviations can be prepared? Repulsion between kinks in adjacent steps of 22 meV has been found for Ag(115) [69]. It is of fundamental interest to study how the interaction energy between kinks falls off with distance along the same step and between adjacent steps. This dependence will eventually determine the maximum size of the supercell which can be used. Is it possible to prevent such structures from destruction, which would result from alloying? The questions are presently open.

Acknowledgments

The authors wish to thank M Blanc, P Gambardella, S Sarbach, and T Y Lee and acknowledge their contributions to the topics presented in this article.

Appendix. Simple model of oscillations due to row-by-row growth

Here we present a simple formalism to model the observed row oscillations in grazing geometry He scattering. The arguments follow the discussion in [24] but with an analytic approach instead of a numerical one.

We assume for the oscillation connected with the creation of one row a nearly parabolic shape shown in figure A.1(a).

$$f_n(\theta) = 1 - |\sin(n\pi\theta)|. \tag{A.1}$$

The period in the adsorbate coverage θ is related to the time necessary to fill up a row, which again depends on the width of the lower terrace next to the step edge expressed by the number of rows n. The number of oscillations during the deposition of one ML is determined by the number n of rows on a given terrace. n can assume positive non-zero integer values. The observed He reflectivity F is modelled as an incoherent superposition of such oscillations

$$F(\theta) = \sum_n f_n(\theta) P(n) \tag{A.2}$$

which is weighted with the Gaussian distribution function of terrace widths

$$P(n) = \frac{1}{N} \exp\left(-\frac{(n - \bar{n})}{2\sigma^2} \right) \tag{A.3}$$

in which the parameters for the terrace width distribution ($\bar{n} = 8, \sigma = 1.2$) from [17] are used and N is a normalization factor for the distribution. In the model all terraces reach ML coverage at the same time so that the coverage can be identified with evaporation time.

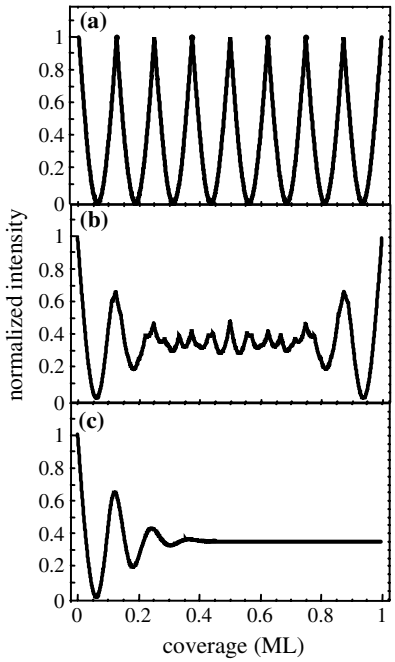

Figure A.1. Simulation of He reflectivity with the simple model described in the appendix. (a) Oscillation with a terrace width of $\bar{n} = 8$ rows and a standard deviation $\sigma = 0$. (b) The same with a mean terrace width of $\bar{n} = 8$ rows and a standard deviation $\sigma = 1.2$ rows using the sum over integer terrace widths given by equation (A.2). (c) The same as (b) but integrating also over non-integer terrace widths using equation (A.4).

It can be seen from figure A.1(b) that the oscillations of $F(\theta)$ are strongly damped and only intensity maxima for the completion of the first two rows can be resolved. After that the oscillations generated by different terraces are losing phase. Due to the coherence of growth phases in (A.2) the model generates a rephasing of the oscillation just before ML completion, which is, however, not observed experimentally. The rephasing results from the fact that a terrace has in the beginning a well defined integer width, and the area which collects the adsorbates attaching to the step edge is assumed to stay constant. In a real growth situation the first condition is not exactly fulfilled due to the presence of kinks, which result in an effective non-integer width in the region adjacent to the kink. The second assumption holds only if the substrate step edge remains the most important diffusion barrier inhibiting adsorbate diffusion.

If we relax the first condition and choose the terrace width n to be a continuous coordinate we may replace the discrete sum by an integral

$$F(\theta) = \int_n f(n, \theta) P(n) \tag{A.4}$$

and obtain the result shown in figure A.1(c). We see that the rephasing of oscillations disappears. The rephasing tendency is weakened even more if the relevant diffusion barrier is assumed to move with the advancing step.

References

[1] Jeong H-C and Williams E D 1999 *Surf. Sci. Rep.* **34** 171
[2] Giesen M, Linke U and Ibach H 1997 *Surf. Sci.* **389** 264

[3] Bartolini A, Ercolessi F and Tosatti E *Phys. Rev. Lett.* **63** 872
[4] Watson G M, Gibbs D, Zehner D M, Yoon M and Mochrie S G J 1993 *Phys. Rev. Lett.* **71** 3166
[5] Moest B, Wouda P T, Denier van der Gon A W, Langelaar M C, Brongersma H H, Nieuwenhuys B E and Boerma D O 2001 *Surf. Sci.* **473** 159
[6] Goapper S, Barbier L, Salanon B, Loiseau A and Torrelles X 1998 *Phys. Rev.* B **57** 12497
[7] Comsa G, Mechtersheimer G and Poelsema B 1982 *Surf. Sci.* **119** 172
[8] Batteas J, Dunphy J, Somorjai G and Salmeron M 1996 *Phys. Rev. Lett.* **77** 534
[9] Walko D A and Robinson I K 1999 *Phys. Rev.* B **59** 15446
[10] Savio L, Vattuone L and Rocca M *Phys. Rev. Lett.* **87** 276101
[11] Folsch S, Helms A, Riemann A, Repp J, Meyer G and Rieder K H 2002 *Surf. Sci.* **497** 113
[12] Levy R A 1968 *Principles of Solid State Physics* (New York: Academic)
[13] Blanc M, Marsico V, Kuhnke K and Kern K 1998 *Surf. Sci. Lett.* **414** L964
[14] Schuster R, Blanc M, Kuhnke K, Robinson I K and Ferrer S 1997 unpublished results
[15] Williams E D and Bartelt N C 1996 Thermodynamics and statistical mechanics of surfaces *Physical Structure* ed W N Unertl (Amsterdam: Elsevier)
[16] Steadman P, Peters K F, Isern H and Ferrer S 2001 *Phys. Rev.* B **64** 125418
[17] Hahn E, Schief H, Marsico V, Fricke A and Kern K 1994 *Phys. Rev. Lett.* **72** 3378
[18] Frenken J W M and Stoltze P 1999 *Phys. Rev. Lett.* **82** 3500
[19] Swamy K, Bertel E and Vilfan I 1999 *Surf. Sci.* **425** L369
[20] Giesen-Seibert M, Jentjens R, Poensgen M and Ibach H 1993 *Phys. Rev. Lett.* **71** 3521
[21] Lapujoulade J 1994 *Surf. Sci. Rep.* **20** 191
[22] Hammonds K D and Lynden-Bell R M 1992 *Surf. Sci.* **278** 437
[23] Robinson I K, Vlieg E and Kern K 1989 *Phys. Rev. Lett.* **63** 2578
[24] Blanc M 1998 *PhD Thesis* EPFL, Lausanne
[25] Röder H, Hahn E, Brune H, Bucher J P and Kern K 1993 *Nature* **366** 141
[26] Brune H 1998 *Surf. Sci. Rep.* **31** 121
[27] Krug J 2002 *Physica* A **313** 47
[28] Gambardella P, Sljivancanin Z, Hammer B, Blanc M, Kuhnke K and Kern K 2001 *Phys. Rev. Lett.* **87** 056103
[29] Shen J, Skomski R, Klaua M, Jenniches H, Manoharan S S and Kirschner J 1997 *Phys. Rev.* B **56** 2340
[30] Marsico V, Blanc M, Kuhnke K and Kern K 1997 *Phys. Rev. Lett.* **78** 94
[31] Alnot M, Barnard J A, Ehrhardt J J and Mutaftschiev B 1990 *J. Cryst. Growth* **102** 629
[32] Bott M, Michely T and Comsa G 1992 *Surf. Sci.* **272** 161
[33] Röder H, Brune H, Bucher J P and Kern K 1993 *Surf. Sci.* **298** 121
[34] Bales G S and Zangwill A 1990 *Phys. Rev.* B **41** 5500
[35] Máca F, Kotrla M and Trushin O S 1999 *Vacuum* **54** 113
[36] Leonardelli G, Lundgren E and Schmid M 2001 *Surf. Sci.* **490** 29
[37] Basset D W and Webber P R 1978 *Surf. Sci.* **70** 520
[38] Goelzhaeuser A and Ehrlich G 1997 *Z. Phys. Chem.* **202** 59
[39] Kunkel R, Poelsema B, Verheij L K and Comsa G 1990 *Phys. Rev. Lett.* **65** 733
[40] Feibelman P J 1999 *Phys. Rev.* B **60** 4972
[41] Kyuno K, Gölzhäuser A and Ehrlich G 1998 *Surf. Sci.* **397** 191
[42] Bott M, Hohage M, Morgenstern M, Michely T and Comsa G 1996 *Phys. Rev. Lett.* **76** 1304
[43] Boisvert G, Lewis L J and Scheffler M 1998 *Phys. Rev.* B **57** 1881
[44] Gambardella P and Kern K 2001 *Surf. Sci.* **475** L229
[45] van Gastel R, Somfai E, van Albada S B, van Saarloos W and Frenken J W M 2001 *Phys. Rev. Lett.* **86** 1562
[46] Brune H, Röder H, Boragno C and Kern K 1994 *Phys. Rev. Lett.* **73** 1955
[47] Feibelman P J 1994 *Surf. Sci.* **313** L801
[48] Gambardella P, Blanc M, Kuhnke K, Kern K, Picaud F, Ramseyer C, Girardet C, Barreteau C, Spanjaard D and Desjonquères M C 2001 *Phys. Rev.* B **64** 045404
[49] Röder H, Bromann K, Brune H and Kern K 1997 *Surf. Sci.* **376** 13
[50] Picaud F, Ramseyer C, Girardet C and Jensen P 2000 *Phys. Rev.* B **61** 16154
[51] Gambardella P, Blanc M, Bürgi L, Kuhnke K and Kern K 2000 *Surf. Sci.* **449** 93
[52] Lee T Y, Sarbach S, Kuhnke K and Kern K, in preparation
[53] Basset D W 1995 *Surf. Sci.* **325** 121
[54] Christensen A, Ruban A V, Stoltze P, Jacobsen K W, Skriver H L and Nørskov J K 1997 *Phys. Rev.* B **56** 5822
[55] Röder H, Schuster R, Brune H and Kern K 1993 *Phys. Rev. Lett.* **71** 2086
[56] Gambardella P, Dallmeyer A, Maiti K, Malagoli M C, Eberhard W, Kern K and Carbone C 2002 *Nature* **416** 301

[57] Wildberger K, Stepanyuk V S, Lang P, Zeller R and Dederichs P H 1995 *Phys. Rev. Lett.* **75** 509
[58] Hammer B 1999 *Phys. Rev. Lett.* **83** 3681
[59] Weinelt M, Trischberger P, Widdra W, Eberle K, Zebisch P, Gokhale S, Menzel D, Henk J, Feder R, Droge H and Steinruck H-P 1995 *Phys. Rev.* B **52** R17048
[60] Nilius N, Wallis T M and Ho W 2002 *Science* **297** 1853
[61] Dallmeyer A, Carbone C, Eberhardt W, Pampuch C, Rader O, Gudat W, Gambardella P and Kern K 2000 *Phys. Rev.* B **61** R5133
[62] Lin J-L, Petrovykh D Y, Kirakosian A, Rauscher H, Himpsel F J and Dowben P A 2001 *Appl. Phys. Lett.* **78** 829
[63] Fukui T 1992 *J. Cryst. Growth* **124** 493
[64] Sundarm M, Chalmers S, Hopkins P and Gossard C 1991 *Science* **254** 1326
[65] Weiss W and Ritter M 1999 *Phys. Rev.* B **59** 5201
[66] Gambardella P 2000 *PhD Thesis* EPFL, Lausanne
[67] Holst B, Nohlen M, Wandelt K and Allison W 1997 *Surf. Sci.* **377–379** 891
[68] Horvath J and Gellman A 2002 *J. Am. Chem. Soc.* **124** 2384
[69] Hoogeman M S, Schlößer D C, Sanders J B, Kuipers L and Frenken J W M 1996 *Phys. Rev.* B **53** R13299